Atmospheric Environment 64 (2013) 95–102

Contents lists available at SciVerse ScienceDirect

Atmospheric Environment

journal homepage: www.elsevier.com/locate/atmosenv

Trend analysis of atmospheric deposition data: A comparison of statistical approaches

Aldo Marchetto*, Michela Rogora, Silvia Arisci

CNR Istituto per lo Studio degli Ecosistemi, Largo Tonolli 50, 28922 Verbania Pallanza, Italy

HIGHLIGHTS

- We used numerical simulation and deposition data to compare trend analysis techniques.
- The Seasonal Kendall Test showed the highest power.
- Its power was increased when using weekly data instead of pooling the samples.

ARTICLE INFO

Article history:
Received 24 April 2012
Received in revised form
20 July 2012
Accepted 11 August 2012

Keywords:
Trend
Atmospheric deposition
Kendall test

ABSTRACT

Numerical simulation was used to compare the most used trend analysis techniques on data series of ionic concentrations in atmospheric deposition. The Seasonal Kendall Test (SKT) showed the highest power, which increased in particular when using original weekly data instead of pooling together the samples in monthly or yearly volume-weighted averages. The simulation also showed that differences in power among tests and pooling intervals would be negligible for data series longer than about 12 years.

We tested these results using data from a network of bulk deposition samplers at nine forest sites in Italy, for which data have been available since 1998. These sites were selected in different forests, ranging from arid Mediterranean evergreen oak forest to rainy Alpine beech or spruce forests. The results showed relevant differences as regards the number of significant trends detected using different techniques and different data pooling, even for 13-year data series.

The use of minimum–maximum autocorrelation factor analysis allowed a better interpretation of the data, showing the main trend shapes among stations and variables.

1. Introduction

During the 20th century, large regions of Europe received elevated deposition of nitrogen (N) and sulphur (S) compounds due to the emission of N and S oxides from combustion of fossil fuels and the emission of ammonia from agriculture and stock rearing. Sulphur oxide emission reached its maximum level by about 1980, thereafter decreasing steadily in most countries (Tarrason and Schaug, 2000). In contrast, N emission control started later and N decrease was slighter and slower (Fagerli and Aas, 2008).

In the atmosphere, N and S oxides and ammonia are transformed into nitric and sulphuric acid, and ammonium, respectively. In these forms, they can be transported over hundreds of kilometres and reach remote ecosystems in the form of particulate matter (dry deposition), rain, or snow (wet deposition). In Italy, a network of forest sites for monitoring the effect of air pollution on forests was set up in 1995 (Petriccione and Pompei, 2002), as part of Italy's contribution to the UN-ECE Convention on Long Range Transboundary Air Pollution. Monitoring of atmospheric deposition started in 1998 (Mosello et al., 2002).

A number of techniques have been used to detect statistically significant trends in the composition of atmospheric deposition, such as time series analysis (Kessler et al., 1992; Terry et al., 1986; Civerolo and Rao, 2001; Sirois et al., 2001; Temme et al,. 2004) or general linear models (Lynch et al., 1995). However, a large majority of the studies used either the Mann–Kendall test (MKT: Mann, 1945) (e.g. Aherne et al., 2010; Waller et al., 2012), the seasonal Kendall test (SKT: Hirsch et al., 1982) (e.g. Mosello et al., 1992; Lehmann et al., 2005; Webster and Brezonik, 1995; Nilles and Conley, 2001; Bruns, 2003; Prestbo and Gay, 2009) or a linear regression of annual averages vs time (e.g., Summers, 1995;

Abbreviations: MKT, Mann–Kendall test; SKT, Seasonal Kendall test; MAFA, Minimum–maximum autocorrelation factor analysis; TN, Total nitrogen; SDL, standard deviation of the log-transformed data.

* Corresponding author. Tel.: +39 0323 518331; fax: +39 0323 556513.
E-mail address: a.marchetto@ise.cnr.it (A. Marchetto).

1352-2310/$ – see front matter © 2012 Elsevier Ltd. All rights reserved.
http://dx.doi.org/10.1016/j.atmosenv.2012.08.020

Kopacek et al., 1997; Puxbaum et al., 1998; Huang et al., 2008; Lloyd, 2010).

Time series analysis has the potential for building predictive models; the common use of MKT and SKT is partly due to their power to detect trend in time series with multiple missing data, values below detection limits (Helsel, 2005) and strong seasonality (Hirsch et al., 1982), and to the possibility to elaborate large data sets in a standard way.

Combining results from several sites into regional or national trends can give an overall indication of temporal changes in the chemistry of deposition, for example to evaluate the effect of emission reduction at a country level. In this case, a procedure combining different tests may allow the detection of a consistent trend over an entire region.

In this paper, we use numerical simulation to compare the power of the most used trend analysis techniques (MKT, SKT and linear regression). These tests were applied on simulated weekly, monthly and yearly data, in order to understand the effect of data pooling on the power of the statistical tests. We then applied the SKT and linear regression to assess trends in the chemistry of bulk deposition at 9 forest sites in Italy, for which data have been available since 1998, in order to verify our results on actual data sets.

Finally, we discussed common trends among stations and variables using the minimum-maximum autocorrelation factor analysis (MAFA: Shapiro and Switzer, 1989; Solow, 1994), to get an overall picture of temporal trends at a regional or national scale.

2. Methods

2.1. Atmospheric deposition data

Samples for the determination of atmospheric deposition chemistry were taken in nine sites (Fig. 1 and Table 1), ideally located in large homogeneous forest areas (Petriccione and Pompei, 2002). Three bulk collectors are located in the open field, in a clearing close to the sampling area. The collector is a 2-l graduated polyethylene bottle, with a funnel of 19.5 cm diameter. A polyethylene net in the funnel prevents the collection of coarse debris, insects and leaves, while a metal ring above the funnel has the function of avoiding bird droppings. The bottle is shaded by a PVC cylinder.

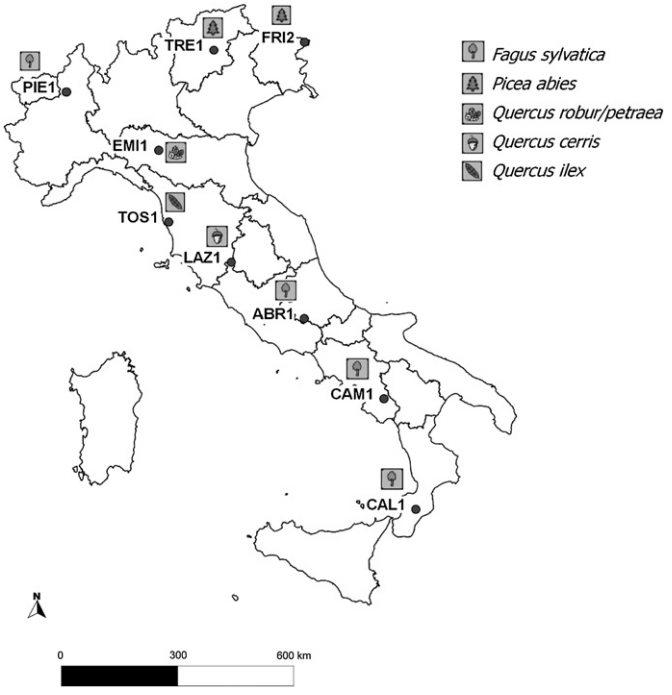

Fig. 1. Location of study sites and vegetation types.

Table 1
Selected features and main dominant tree species in the study sites.

Site	Code	Altitude a.s.l. (m)	Mean annual temp. (°C)	Lithological substrate	Dominant tree species
Selva Piana (AQ)	ABR1	1500	10	Limestone	*Fagus sylvatica*
Piano Limina (RC)	CAL1	1100	10	Granite	*Fagus sylvatica*
Corleto Monforte (SA)	CAM1	1175	10	Limestone	*Fagus sylvatica*
Boschi Carrega (PR)	EMI1	200	12	Ancient alluvium	*Quercus robur* *Quercus petraea*
Tarvisio (UD)	FRI2	820	6	Phyllites	*Picea abies*
Monte Rufeno (VT)	LAZ1	690	12	Sandstone flisch	*Quercus cerris*
Val Sessera (BI)	PIE1	1150	8	Micaschist	*Fagus sylvatica*
Colognole (LI)	TOS1	150	15	Gabbro	*Quercus ilex*
Passo Lavazè (TN)	TRE1	1775	5	Granite	*Picea abies*

Every Tuesday, samples are collected and collecting funnels and bottles washed with de-ionized water. Volume measurements are performed in the field and then the individual samples are pooled together into one weekly sample, an aliquot of which is sent to the laboratory. Since 1999, snow sampling has been carried out using cylindrical PVC containers (diameter = 20 cm, height = 80 cm).

Conductivity and pH are measured on unfiltered samples. All other analyses are performed on filtered samples (0.45 μm). Sulphate, chloride, nitrate, sodium, potassium, magnesium and calcium are measured by ion chromatography, ammonium and total nitrogen by spectrophotometry (Fresenius et al., 1988; Valderrama, 1981) and alkalinity by acid titration with two end-points (Rodier, 1981). Reactive phosphorus is also measured by spectrophotometry, to reveal any contamination of the samples by bird droppings.

Analytical quality assurance and control are provided by the use of control charts for all variables, the check of ion balance and conductivity (Mosello et al., 2005, 2008) and regular participation in international intercomparison exercises, such those organized within the "ICP Waters" (Kvaeven et al., 2001) and "ICP Forests" (Marchetto et al., 2009) programmes.

For trend analysis, original weekly data were volume-weighted averaged into monthly and yearly values. Average pH values were obtained by the volume-weighted average of H^+ concentration. When calculating monthly data, weeks bridging two months were assigned to both months, in proportion to the number of days belonging to each month.

2.2. Trend analysis

Trend analysis was performed separately on annual, monthly and weekly data.

Linear regression of all variables against time was performed directly on Excel data sheets.

MKT and SKT were performed using the R software and the function reported in the Appendix, which also estimates trend slopes, according to Sen (1968).

MKT is an application to time series of Kendall's Tau test using time as the independent variable. MKT is a test for monotonic trends, first suggested by Mann (1945).

Assuming that a time series is formed by n data (Y_1, Y_2, $Y_{3,\ldots}$ Y_n), Kendall's S statistic is computed from each data pair:

$$S = P - N$$

where P is the number of $Y_i < Y_j$ for all $i < j$ and N is the number of $Y_i > Y_j$ for $i < j$.

S has expectation zero and variance

$$\sigma^2 = \left[n(n-1)(2n+5) - \sum t_i(t_i-1)(2t_i-5)\right] \Big/ 18$$

where t_i is the number of data involved in any given tie.

SKT is an extension of MKT, insensitive to seasonality, in which the data set is split into g separate time series, one for each month or season, and the test statistic is the sum of Kendall's S statistics calculated for each of these g time series. Hirsch et al. (1982) showed that, using a continuity correction, SKT can be used for short time series ($n = 3$). Hirsch and Slack (1984) further developed the test to account for covariance among seasons. SKT is implemented in a number of software packages, but not all of them use the complete formulation, correcting for ties and covariance among seasons. An example of the complete implementation is given by Helsel et al. (2006), and by the R function reported in the Appendix.

2.3. Numerical simulations

The statistical power of different techniques for trend analysis was compared using Monte-Carlo simulation. Weekly data with a trend and/or seasonality were generated, and the different tests applied to each simulation to determine if the individual methods can detect the trend. The simulation is repeated 10,000 times in a Monte-Carlo type situation.

A preliminary screening of the data showed that in most cases their distribution is close to log-normal, with standard deviation of the log-transformed (SDL) data ranging from 0.2 to 0.5. Simulated data were then generated using the R software (R Development Core, 2005), assuming log-normal distribution.

For the sake of simplicity, weekly data were approximated by 48 points per year. Monthly and yearly averages were obtained by averaging 4 and 48 consecutive points, respectively.

A seasonal pattern was added by multiplying each value by one half of a sinus function with a yearly period. Finally, a linear trend was added to each simulated data set.

Both MKT and SKT were performed on weekly and monthly data, using the function reported in the Appendix. MKT and linear regression were applied to annual averages.

The number of times that a significant ($p < 0.05$) trend was detected was then used as an estimation of the power of each test.

We performed a number of simulations, varying (i) the slope of the trend, (ii) the standard deviation of the random distribution of the data points, (iii) the length of the data series, and (iv) including or not the seasonality.

Four groups of simulation are shown in this paper (Table 2): in the first group, summarized in Fig. 2, the seasonal effect was not considered, SDL was fixed to 0.3 and length of the time series to 12 years, while the trend slope varied from 0.5 to 3% y^{-1}. In the second group (Fig. 3), the seasonal effect was added, multiplying each simulated datum by a sinusoidal function with a 1-year period. The seasonal effect was also added in the third group of simulations (Fig. 4), the length of the time series (12 years) and the trend slope (2% y^{-1}) were fixed, but with SDL ranging between 0 and 1. Finally, the last group of simulations (Fig. 5), still including the seasonal effect, was performed at variable time series lengths (5–15 years), and fixed SDL (0.3) and slope (2% y^{-1}). Each point in Figs. 2–5 represents 10,000 simulations.

Table 2
List of simulation groups performed. Each point in Figs. 2–5 represents 10,000 simulations.

No.	Seasonality	Standard deviation	Length (y)	Trend slope (y^{-1})	No. of points	Figure
1	No	0.3	12	0.5–3%	26	2
2	Yes	0.3	12	0.5–3%	26	3
3	Yes	0–1	12	2%	11	4
4	Yes	0.3	5–15	2%	11	5

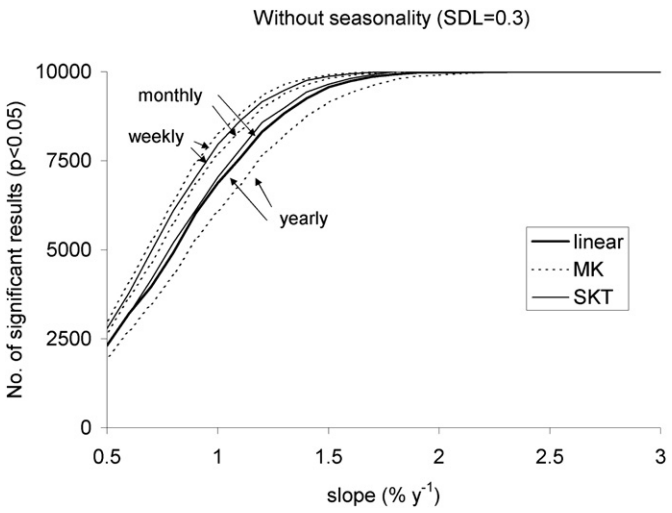

Fig. 2. Results of the numerical simulation, not including seasonal effect, with fixed SDL (0.3) and length of the time series (12 years), but varying the trend slope.

2.4. Slope estimation

Trend slopes were estimated following Sen (1968), as the median of the slope determined by all pairs of sample points, excluding points with equal time coordinates. As proposed by Hirsch et al. (1982), only pairs of points belonging to the same month were considered, in order to minimize the effect of seasonality.

2.5. Common trends

The temporal pattern of the detected common trends was investigated through minimum-maximum autocorrelation factor

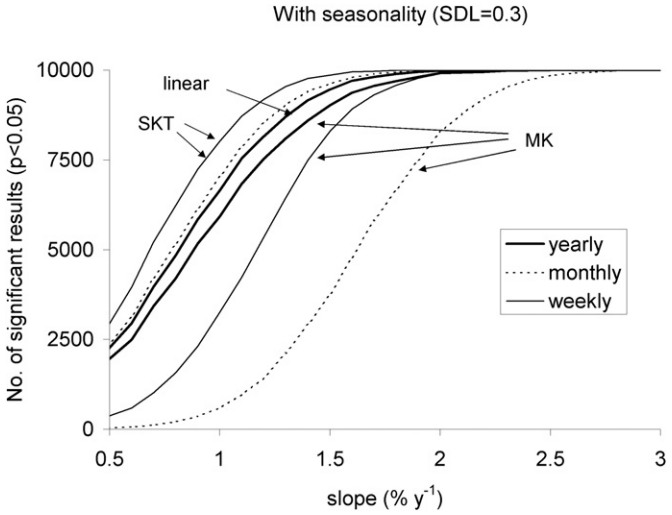

Fig. 3. Results of the numerical simulation including seasonal effect, with fixed SDL (0.3) and length of the time series (12 years), but varying the trend slope.

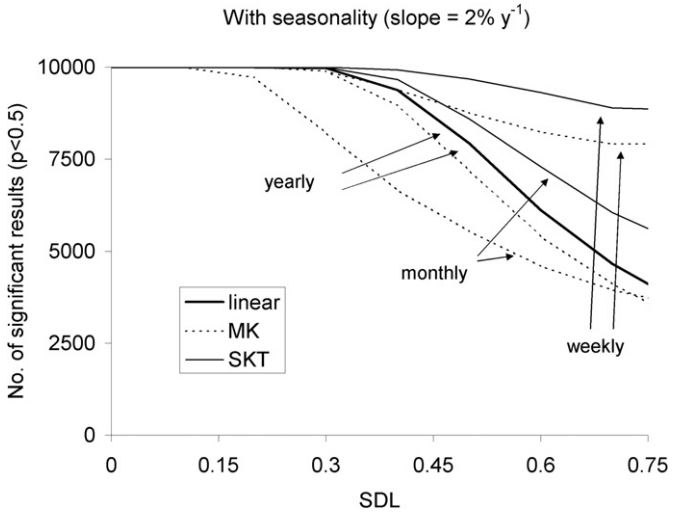

Fig. 4. Results of the numerical simulation including seasonal effect, with fixed length of the time series (12 years) and trend slope (2% y^{-1}), but varying SDL.

analysis (MAFA: Shapiro and Switzer, 1989; Solow, 1994) applied to monthly data, using the *Brodgar* software vers. 2.5.1 (Highland. Statistics Ltd). This technique can be used to extract the main trends from multivariate time series. Monototonic trends are detected by SKT, while the results of MAFA can be used to assess the presence of short-term increases and/or decreases and the general temporal pattern.

To assess the statistical significance of MAFA axes, the randomisation process described by Solow (1994) was used. The significance of the correlation between each axis of the MAFA and the concentration time series was also tested.

3. Results and discussion

3.1. Numerical simulations

Considering a long data series, composed of twelve years of data, the powers of the different tests compare quite well, if data are randomly distributed without a marked seasonal variability. The simulation results shown in Fig. 2 indicate that the use of weekly rather than monthly data slightly improve the power of the test. The power of the MKT applied to monthly data is similar to that of a linear regression carried out on annual means. In contrast, the power of MKT on annual data is lower.

The pattern changes considerably if the seasonal effect is added to the simulated data (Fig. 3). With a relatively low logarithmic SD (0.2 log units), the power of SKT is markedly higher than those of the MKT. Again, the power of the MKT run on monthly data is similar to that of a linear regression carried out on annual means. However, with increasing variability (SDL > 0.5), the advantage of the SKT run on monthly data vs the linear regression on annual values becomes evident (Fig. 4).

The results shown refer to relatively long time series, comparable to those usually available in the ICP Forests programme or in other monitoring programmes of atmospheric deposition chemistry. For shorter data series, the advantage of the SKT becomes evident even when SLD is relatively low, such as, for example, SDL = 0.3 (Fig. 5).

From the overall results, it can be concluded that SKT is the more suitable technique to be applied to data commonly used in trend analysis. The use of weekly rather than monthly data would further improve the power of the test.

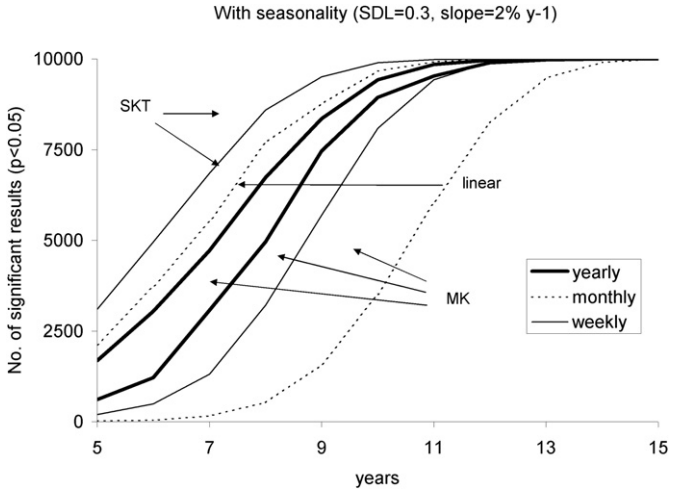

Fig. 5. Results of the numerical simulation including seasonal effect, with fixed SDL (0.3) and trend slope (2% y^{-1}), but varying the length of the time series.

3.2. Status of atmospheric deposition in Italian forest sites

The mean volume-weighted concentration values of the period 2009–2010 for some selected ions, pH, conductivity, alkalinity, total nitrogen and the amount of precipitation are presented in Table 3. The amounts of precipitation range between 1054 and 2091 mm y^{-1}, with the highest value recorded at PIE1 in the Western Alps, and the lowest at EMI1, in central Italy. In all sites, average pH values are higher than 5.0. The mean annual concentrations of NH_4^+ and NO_3^- show wide variations among sites, with NH_4^+ ranging between 10 μeq L^{-1} (CAL1) and 49 μeq L^{-1} (EMI1) and NO_3^- between 10 μeq L^{-1} (CAL1) and 36 μeq L^{-1} (EMI1). This latter site, where high NH_4^+ and NO_3^- concentrations were registered, is close to the Po Plain, a large area characterized by high emissions deriving from agriculture and industry. Other sites with high NO_3 concentrations, like PIE1, lie on the Southern slope of the Alps, where they receive depositions originating from wet air masses coming northward from the Mediterranean Sea and crossing the industrial areas in the Po Plain (Mosello et al., 1992; Rogora et al., 2006).

High values of $SO_4^=$ were measured at CAL1 (34 μeq L^{-1}) and LAZ1 (30 μeq L^{-1}), while for the other sites the range was between 5 μeq L^{-1} (FRI2) and 10–15 μeq L^{-1} (TRE1, PIE1). For Ca^{++} and Mg^{++} concentrations, the ranges are 6–67 μeq L^{-1} and 3–27 μeq L^{-1} respectively, with lower values at the alpine sites and higher values in the central-southern regions. Most of these ions derive from the long-range transport of Saharan dust, which is more important at the southernmost sites. Calcium is in general the main cation at all the sites, followed by sodium, magnesium and potassium. Higher values of magnesium and sodium are recorded in the sites closer to the sea, due to the contribution of sea spray (e.g. TOS1, CAL1, CAM1). Total nitrogen range is 34–90 μM, with the highest values at EMI1, PIE1, and LAZ1, and the lowest at the southern sites and in the north-eastern Alps (Table 3).

3.3. Comparison of statistical approaches on the observed data

The results of the comparison using both Kendall tests and linear regression on weekly, monthly and yearly data for the period 1998–2010 are shown in Table 4. MKT was used for yearly data, while SKT was used for monthly and weekly data.

Table 3
Amount of precipitation (mm) and volume-weighted mean concentrations (2009–2010) of main ions (μeq L^{-1}), pH, conductivity (Cond., μS cm^{-1} at 20 °C), alkalinity (Alk, μeq L^{-1}) and total nitrogen (TN, μM) in open field deposition.

Open field	mm	pH[a]	Cond.	NH_4^+	Ca^{++}	Mg^{++}	Na^+	K^+	Alk	$SO_4^=$	NO_3^-	Cl^-	TN
ABR1	1469	5.8	13.1	15	51	13	31	3	37	22	17	32	37
CAL1	1951	5.5	21.0	10	37	26	93	10	24	34	10	102	34
CAM1	1263	5.8	19.9	13	58	22	75	4	33	37	16	83	35
EMI1	1054	5.7	13.3	49	27	6	15	5	28	22	36	14	90
FRI2	1856	5.5	8.2	44	6	17	6	5	25	5	22	1	37
LAZ1	1149	5.8	21.7	15	67	25	65	20	42	30	29	77	56
PIE1	2091	5.2	8.2	26	8	3	7	2	5	15	24	5	57
TOS1	1317	5.3	22.1	15	39	27	91	8	20	31	25	100	46
TRE1	1063	5.6	6.9	15	16	6	7	2	16	10	14	6	37

[a] pH calculated from the weighted mean of H^+ concentration.

Table 4 resumes the results of a large number of tests, performed without any correction for multiple comparison. To reduce the probability of false positives, trends were considered as significant with a probability level of $p < 0.001$.

All tests revealed a highly significant decrease in $SO_4^=$ concentration for most sites, but the number of significant trends detected for the other variables using different tests and data sets were sharply different. In good agreement with the simulation data, linear regression and MKT on annual data detected a lower number of significant trends than SKT.

In spite of the restrictive probability level used, SKT used on both monthly and weekly data detected a large number of significant trends, in particular for base cations (Ca^{++}, Mg^{++}, Na^+, K^+), the deposition of which is more episodic (Rogora et al., 2004). In the case of sulphate, the gradual implementation of measures for controlling SO_2 emission led to a regular trend on a long time period, but also in this case SKT detected more significant trends on monthly data than linear regression.

Our results confirm the importance of using the MKT and SKT for the detection of monotonic trends, as suggested in previous papers (e.g. Bruns, 2003; Pannatier et al., 2011).

Surprisingly, we obtained a large increase in the number of detected trends using weekly data instead of monthly data, with both linear regression and the Kendall tests (Table 4), even if the advantage of using SKT is still evident. This result does not completely agree with the simulations, which showed that with 13 years of data the power of the different methods should be comparable.

However, our data series contain a relevant number of outliers, because of samples with low deposition amount and high concentration of the major ions, or because of the episodic deposition of Saharan dust (Rogora et al., 2004). In these conditions, the advantage of SKT, in particular with weekly data, is considerable.

Based on these results, SKT and weekly data will be used in the next paragraph.

Table 4
Number of significant ($p < 0.001$) trends detected using different statistical techniques and data aggregation.

Variable	Linear regression			SKT		MKT
	Weekly data	Monthly data	Yearly data	Weekly data	Monthly data	Yearly data
Amount (mm)	0	1	0	1	0	1
pH	0	2	0	2	2	1
Ca	3	1	1	6	5	0
Mg	4	2	0	9	4	0
Na	2	0	0	5	0	1
K	4	2	1	9	6	1
Ammonium	2	1	0	6	2	0
Sulphate	8	6	5	8	9	6
Nitrate	2	0	0	7	2	0
Chloride	1	0	0	4	1	0
Total N	4	0	1	6	4	0
Total number of detected trends	30	15	8	63	35	10

3.4. Rate of change

Trend slopes were estimated on the basis of weekly data, following Sen (1968), and considering pairs of points belonging to the same month (Hirsch and Slack, 1984). Slopes were calculated and discussed only if SKT detected a significant ($p < 0.001$) trend for that particular time series.

A negative trend for sulphate was found at all sites, with slope values ranging between −1.4 and −3.4 μeq L^{-1} y^{-1}. Other significant results emerged for Ca^{++}, Mg^{++} and K^+, showing a decreasing trend. Nitrate significantly decreased at seven out of nine sites. This pattern compares with the recent reduction in the emissions of nitrogen oxides (WebDab, 2011), but only two significant trends would have been detected by performing SKT on monthly data (Table 5). Six sites also showed significant negative trends of NH_4^+ and TN.

3.5. Common trend shape

The minimum-maximum autocorrelation factor analysis (MAFA), as described in Shapiro and Switzer (1989) and Solow (1994), was applied to monthly concentrations for the period 1998–2010, considering the following variables: Ca^{++}, Mg^{++}, TN, NH_4^+, NO_3^-, and SO_4^{--}.

This technique was included in order to extract the main trend pattern, including the presence of short-term increases and/or decreases, which can not be detected by SKT.

Table 5
Sen's slopes of monthly concentrations of the period 1998–2010 (μeq L^{-1} y^{-1}, TN μM, pH units y^{-1}). Significant trends (SKT, $p < 0.001$) in bold.

Open field	ABR1	CAL1	CAM1	EMI1	FRI2	LAZ1	PIE1	TOS1	TRE1
mm	0.88	0.00	0.89	0.19	0.43	−0.16	**−0.43**	0.54	−0.50
pH	−0.04	0.01	−0.01	0.02	0.01	0.01	**0.02**	0.01	**−0.04**
Ca^{++}	**−4.82**	−0.66	**−2.30**	−1.79	**−0.72**	−1.02	**−0.98**	**−2.20**	**−2.16**
Mg^{++}	**−0.64**	**−0.22**	**−0.85**	**−0.53**	**−0.14**	**−0.28**	**−0.09**	**−0.64**	**−1.06**
Na^{++}	−0.62	−0.51	−1.53	**−0.69**	**0.003**	−0.63	**−0.05**	**−3.46**	**−0.27**
K^+	**−0.33**	**−0.23**	**−0.34**	**−0.29**	**−0.13**	**−0.18**	**−0.15**	**−0.34**	**−0.31**
NH_4^+	**−1.00**	**−0.33**	−0.73	−1.13	**−0.66**	**−0.34**	−0.30	**−1.78**	**−0.69**
SO_4^-	**−2.38**	**−1.57**	−1.79	**−3.36**	**−1.53**	**−1.94**	**−1.71**	**−3.09**	**−1.39**
NO_3^-	**−1.79**	**−0.92**	−0.93	**−1.15**	**−0.65**	**−0.49**	−0.73	**−0.26**	**−0.58**
Cl^-	−0.78	−0.33	−1.76	**−0.68**	**0.002**	−0.32	**−0.10**	−1.06	**−0.39**
TN	**−3.96**	**−1.94**	−3.00	**−4.65**	**−1.90**	−1.83	−1.72	**−4.44**	**−2.47**

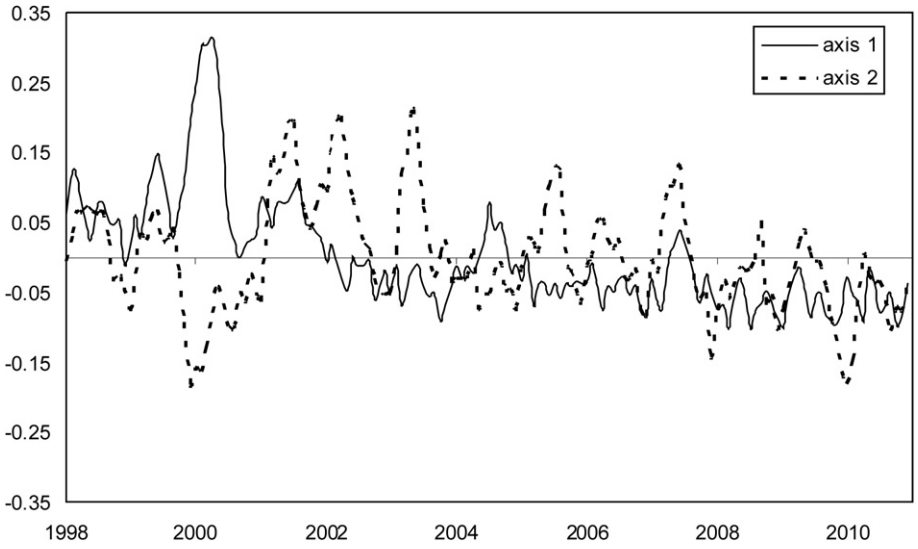

Fig. 6. Main axes extracted by means of min–max factor analysis (MAFA) applied to monthly concentrations of selected variables (Ca, Mg, TN, NH_4, NO_3, SO_4).

Two main axes were extracted from the data set. A randomisation test (Solow, 1994) performed on the ordination showed that both axes are highly significant ($p < 0.001$). These axes represent the main temporal patterns present in the data, and are shown in Fig. 6.

Loadings were also estimated and shown in Table 6, to highlight correlations between each axis and sites/variables.

The first axis represents a decreasing trend, with the steepest decrease within 2001 and 2003; this axis proved to be significantly correlated with sulphate concentration at all the sites, and for TN and NO_3^- at most of them; it was also partly correlated with calcium (4 sites) and magnesium (6 sites) (Table 6).

In fact, sulphate decreased significantly in Europe during the last decades of the 20th century as a result of the reduction in the emission of sulphur compounds after the implementation of the 1985 Helsinki Protocol, and the 1994 Oslo Protocol. In Italy, SO_2 emission decreased by about 60% between 1980 and 2000 (WebDab, 2011). A significant decrease of sulphate concentration in deposition is still in course, as emissions are still decreasing (Amann et al., 2008).

Table 6
Loadings of the MAFA axes (Fig. 6) extracted for each site and for the selected chemical variables. Loadings are in bold for the time series which resulted significantly correlated to the axes.

	Ca^{++}	Mg^{++}	Total N	NH_4^+	NO_3^-	SO_4^{--}
axis 1						
ABR1	**0.1979**	**0.1721**	**0.2421**	**0.2355**	**0.1986**	**0.2243**
CAL1	0.0164	0.1096	0.1182	−0.0951	**0.1822**	**0.1749**
CAM1	**0.1988**	**0.2541**	**0.3000**	0.1094	**0.1697**	**0.3355**
EMI1	0.0627	**0.2201**	0.1150	−0.1158	0.0477	**0.3099**
FRI2	0.0829	0.0675	**0.1966**	0.0380	**0.1915**	**0.3876**
LAZ1	0.1423	**0.3611**	**0.3247**	0.0569	**0.2082**	**0.4822**
PIE1	**0.1697**	**0.226**	**0.2214**	0.0393	**0.2109**	**0.3913**
TOS1	0.1154	0.0747	**0.3205**	**0.2992**	0.0642	**0.3270**
TRE1	**0.4145**	**0.4754**	**0.3347**	**0.1822**	**0.1805**	**0.5575**
axis 2						
ABR1	**0.4441**	**0.3591**	**0.4929**	**0.5587**	**0.4056**	**0.4255**
CAL1	**0.2926**	−0.0177	**0.1752**	**0.1881**	**0.3251**	**0.2921**
CAM1	**0.1787**	−0.0737	**0.4125**	**0.5803**	**0.2158**	**0.1866**
EMI1	**0.3284**	**0.2513**	**0.2853**	**0.2823**	**0.2432**	**0.3564**
FRI2	0.1548	0.0508	**0.4572**	**0.5638**	**0.3380**	**0.5073**
LAZ1	0.1564	**−0.1802**	**0.2432**	**0.4372**	**0.1660**	**0.2056**
PIE1	**0.3498**	**0.2285**	**0.4474**	**0.5182**	**0.2869**	**0.5525**
TOS1	**0.3945**	0.1166	**0.2888**	0.1011	**0.1616**	**0.3046**
TRE1	−0.0065	−0.1263	**0.3058**	**0.3991**	**0.2071**	**0.2542**

The second axis showed a temporary decrease in 2000, followed by a rather steady phase (2001–2003) and then a decreasing trend in 2004–2010; it was significantly correlated with N compounds at most sites, with loadings for TN and NO_3^- higher than those of axis 1 (Fig. 6, Table 6). This is the result of a short-term decrease in 2000 at some of the Alpine sites, due to very high precipitation amounts, and of the decline of N concentration in the last 7 years, because of reduced emissions.

In deposition samples, NO_3 concentrations started to decrease in 2003 (Rogora et al., 2012), with a delay between the reduction in the emission (40% between 1980 and 2010, WebDab, 2011) and the response of the deposition. Such a delay can be due to a number of factors, including changes in the partitioning between wet and dry deposition and changing rates of atmospheric oxidation (Fowler et al., 2007; Irwin et al., 2002). In contrast, the decrease of NH_3 emission in Italy has been small (4% between 1980 and 2010; WebDab, 2011).

4. Conclusions

Our results confirm that the Seasonal Kendall Test (SKT) is particularly useful for the detection of significant trends in deposition series. Simulations show that in the case of series without marked seasonal patterns, the power of SKT is lower than the power of the Mann–Kendall test (MKT). In fact, the former only performs a relatively small number of comparisons between couples of data belonging to the same block (month), while the latter requires a larger number of comparison between all possible couples of data in the time series. However, when seasonality is included, SKT clearly outperforms MKT.

For time series of moderate length (up to ten years), simulations suggest the use of the largest possible number of data (i.e. weekly data when available). With longer series, the advantage of using raw data and of using SKT instead of linear regression disappears.

The application of different tests to a real data set, including 13 years of deposition data collected in nine forested sites in Italy, showed a dramatic increase in the number of detected trends when using SKT. Using both monthly and weekly data, the number of significant trends detected by SKT was more than twice the number detected by linear regression. For measured concentrations, the use of weekly time series instead of monthly data further increased the power of the test.

SKT is a test for monotonic trends, giving no information on their pattern. To get a better picture of the temporal evolution of concentration and deposition, other methods can be used, such as fitting splines to each time series; however, the minimum-maximum autocorrelation factor analysis shows the advantage of making use of all data to produce a summary plot, which can be simply interpreted on the basis of the significant relationships of each time series with the extracted axes.

Our results as a whole confirm the advantage of combining different statistical approaches for the evaluation of temporal trends in atmospheric deposition. The detection of trend as rate of change at a site level and the evaluation of common trends at different sites can be seen as complementary approaches, aiding in the interpretation of the major drivers of change.

Acknowledgements

The long-term collection of deposition data was partially funded by the Italian Forestry Service (Corpo Forestale dello Stato, Servizio CONECOFOR) and by the European Union under the Regulation (EC) No 2152/2003 concerning monitoring of forests and environmental interactions in the community (Forest Focus) and the project LIFE 07 ENV/D/000218 "Further Development and Implementation of an EU-level Forest Monitoring System (FutMon)".

We gratefully acknowledge all operators who have performed sampling in the fields, and Gabriele Tartari, Alfredo Pranzo, Arianna Orrù, Paola Giacomotti, Chiara Manini and Maria Cristina Brizzio for their activity in the laboratory, and Dr. Sandra Spence for the revision of the text.

The suggestions of two anonymous reviewers greatly improved the quality of this manuscript.

Appendix A. Supplementary data

Supplementary data related to this article can be found at http://dx.doi.org/10.1016/j.atmosenv.2012.08.020

References

Aherne, J., Mongeon, A., Watmough, S.A., 2010. Temporal and spatial trends in precipitation chemistry in the Georgia Basin, British Columbia. Journal of Limnology 69 (suppl. 1), 4–10.

Amann, M., Bertok, I., Cofala, J., Heyes, C., Klimont, Z., Rafaj, P., Schöpp, W., Wagner, F., 2008. Baseline emission projections for the revision of the Gothenburg protocol up to 2020. Background paper for the 42nd Session of the Working Group on Strategies and Review of the Convention on Long-range Transboundary Air Pollution, Geneva, September 8–10, 2008.

Bruns, D.A., 2003. Atmospheric nitrogen deposition in the Rocky Mountains of Colorado and southern Wyoming – a review and new analysis of past study results. Atmospheric Environment 37, 921–932.

Civerolo, K., Rao, S.T., 2001. Space-time analysis of precipitation-weighted sulfate concentrations over the eastern US. Atmospheric Environment 35, 5657–5661.

Fagerli, H., Aas, W., 2008. Trends of nitrogen in air and precipitation: model results and observations at EMEP sites in Europe, 1980–2003. Environmental Pollution 154, 448–461.

Fowler, D., Smith, R., Muller, J., Cape, J.N., Sutton, M., Erisman, J.W., et al., 2007. Long term trends in sulphur and nitrogen deposition in Europe and the cause of non-linearities. Water, Air and Soil Pollution, Focus 7, 41–47.

Fresenius, W., Quentin, K.E., Schneider, W., 1988. Water Analysis. Springer-Verlag, Berlin, 804 pp.

Helsel, D.R., 2005. Nondetects and Data Analysis. Statistical for Censored Environmental Data. Kohn Wiley and Son, Hoboken, New Jersey, 250 pp.

Helsel, D.R., Mueller, D.K., Slack, J.R., 2006. Computer Program for the Kendall Family of Trend Tests: U.S. Geological Survey Scientific Investigations Report 2005-5275, 4 pp.

Hirsch, R.M., Slack, J.R., Smith, R.A., 1982. Techniques of trend analysis for monthly water quality data. Water Resources Research 18, 107–121.

Hirsch, R.M., Slack, J.R., 1984. A nonparametric test for seasonal data with serial dependence. Water Resources Research 20, 727–732.

Huang, Y.L., Wang, Y.L., Zhang, L.P., 2008. Long-term trend of chemical composition of wet atmospheric precipitation during 1986–2006 at Shenzhen City, China. Atmospheric Environment 42, 3740–3750.

Irwin, J.G., Campbell, G., Vincent, K., 2002. Trends in sulphate and nitrate wet deposition over the United Kingdom: 1986–1999. Atmospheric Environment 36, 2867–2879.

Kessler, C.J., Porter, T.H., Firth, D., Sager, T.W., Hemphill, M.W., 1992. Factor analysis of trends in Texas acidic deposition. Atmospheric Environment 26A, 1137–1146.

Kopacek, J., Prochazkova, L., Hejzlar, J., Blazka, P., 1997. Trends and seasonal patterns of bulk deposition of nutrients in the Czech Republic. Atmospheric Environment 31, 797–808.

Kvaeven, B., Ulstein, M.J., Skjelkvåle, B.L., Raddum, G.G., Hovind, H., 2001. ICP Waters — an International Programme for Surface Water Monitoring. Water, Air and Soil Pollution 130, 775–780.

Lehmann, C.M.B., Bowersox, V.C., Larson, S.M., 2005. Spatial and temporal trends of precipitation chemistry in the United States, 1985–2002. Environmental Pollution 135, 347–361.

Lloyd, P.J., 2010. Changes in the wet precipitation of sodium and chloride over the continental United States, 1984–2006. Atmospheric Environment 44, 3196–3206.

Lynch, J.A., Grimm, J.W., Bowersox, V.C., 1995. Trends in precipitation chemistry in the United-States – a national perspective, 1980–1992. Atmospheric Environment 29, 1231–1246.

Mann, H.B., 1945. Non-parametric tests against trend. Environmetrica 13, 245–259.

Marchetto, A., Mosello, R., Tartari, G., Tornimbeni, O., Derome, J., Derome, K., Sorsa, P., Konig, N., Clarke, N., Ulrich, E., Kowalska, A., 2009. Influence of QA/QC procedures on non-sampling error in deposition monitoring in forests. Journal of Environmental Monitoring 11, 745–750.

Mosello, R., Della Lucia, M., Marchetto, A., Tartari, G.A., 1992. Trends in the chemistry of surface water in north-western Italy. I. Atmospheric deposition. Memorie dell'Istituto Italiano di Idrobiologia 51, 147–165.

Mosello, R., Brizzio, C., Kotzias, D., Marchetto, A., Rembges, D., Tartari, G.A., 2002. The chemistry of atmospheric deposition in Italy in the framework of the National Programme for Forest Ecosystems Control (CON.ECO.FOR.). Journal of Limnology 61 (Suppl. 1), 77–92.

Mosello, R., Amoriello, M., Amoriello, T., Arisci, S., Carcano, A., Clarke, N., Derome, J., Koenig, N., Tartari, G.A., Ulrich, E., 2005. Validation of chemical analyses of atmospheric deposition in forested European sites. Journal of Limnology 64, 93–102.

Mosello, R., Amoriello, T., Benham, S., Clarke, N., Derome, J., Derome, K., Genouw, G., Koenig, N., Orru, A., Tartari, G., Thimonier, A., Ulrich, E., Lindroos, A.J., 2008. Validation of chemical analyses of atmospheric deposition on forested sites in Europe: 2. DOC concentration as an estimator of the organic ion charge. Journal of Limnology 67, 1–14.

Nilles, M.A., Conley, B.E., 2001. Changes in the chemistry of precipitation in the United States, 1981–1998. Water, Air and Soil Pollution 130, 409–414.

Petriccione, B., Pompei, E., 2002. The CONECOFOR Programme: general presentation aims and co-ordination. Jorunal of Limnology 61 (Suppl. 1), 3–11.

Pannatier, E.G., Thimonier, A., Schmitt, M., Walthert, L., Waldner, P., 2011. A decade of monitoring at Swiss Long-Term Forest Ecosystem Research (LWF) sites: can we observe trends in atmospheric acid deposition and in soil solution acidity? Environmental Monitoring and Assessment 174, 3–30.

Prestbo, E.M., Gay, D.A., 2009. Wet deposition of mercury in the US and Canada, 1996–2005: results and analysis of the NADP mercury deposition network (MDN). Atmospheric Environment 43, 4223–4233.

Puxbaum, H., Simeonov, V., Kalina, M.F., 1998. Ten years trends (1984–1993) in the precipitation chemistry in Central Austria. Atmospheric Environment 32,193–202.

R Development Core Team, 2005. R: A Language and Environment for Statistical Computing, Reference Index Version 2.2.1. R Foundation for Statistical Computing, Vienna, Austria, ISBN 3-900051-07-0.

Rodier, J., 1981. L'analyse de l'eau. Dunod, Paris, 1365 pp.

Rogora, M., Mosello, R., Marchetto, A., 2004. Long-term trends in the chemistry of atmospheric deposition in Northwestern Italy: the role of increasing Saharan dust deposition. Tellus B 56, 426–434.

Rogora, M., Mosello, R., Arisci, S., Brizzio, M.C., Barbieri, A., Balestrini, R., Waldner, P., Schmitt, M., Stähli, M., Thimonier, A., Kalina, M., Puxbaum, H., Nickus, U., Ulrich, E., Probst, A., 2006. An overview of atmospheric deposition chemistry over the Alps: present status and long-term trends. Hydrobiologia 562, 17–40.

Rogora, M., Marchetto, A., Arisci, S., 2012. The role of nitrogen deposition in the recent nitrate decline in lakes and rivers in Northern Italy. Science of Total Environment 417–418, 214–223.

Sen, P.K., 1968. Estimates of the regression coefficient based on Kendall's tau. Journal of the American Statistical Society 63, 1379–1389.

Shapiro, D.E., Switzer, P., 1989. Extracting Time Trends from Multiple Monitoring Sites. Technical Report No. 132. Department of Statistics, Standford University, California.

Sirois, A., Vet, R., MacTavish, D., 2001. Atmospheric deposition to the Turkey lakes watershed: temporal variations and characteristics. Ecosystems 4, 503–513.

Solow, A.R., 1994. Detecting change in the composition of a multispecies community. Biometrics 50, 556–565.

Summers, P.W., 1995. Time trend of wet deposition acidifying potential at five ecological monitoring sites in eastern Canada 1981 – 1993. Water, Air and Soil Pollution 85, 653–658.

Tarrason, L., Schaug, J., 2000. Transboundary Acidification and Eutrophication in Europe. EMEP Summary Report 2000. EMEP/MSC-W 1/2000. Norwegian Meteorological Institute, Oslo, Norway, 264 pp.

Temme, C., Ebinghaus, R., Einax, J.W., Steffen, A., Schroeder, H., 2004. Time series analysis of long-term data sets of atmospheric mercury concentrations. Analytical and Bioanalytical Chemistry 380, 493–501.
Terry, W.R., Lee, J.B., Kumar, A., 1986. Time series analysis in acid rain modeling: evaluation of filling missing values by linear interpolation. Atmospheric Environment 20, 1941–1945.
Valderrama, J.C., 1981. The simultaneous analysis of total nitrogen and total phosphorus in natural waters. Marine Chemistry 10, 109–122.
Waller, K., Driscoll, C., Lynch, J., Neewcomb, D., Roy, K., 2012. Long-term recovery of lakes in the Adirondack region of New York to decreases in acidic deposition. Atmospheric Environment 46, 56–64.
WebDab, 2011. EMEP Activity Data and Emission Database. Available at: http://www.ceip.at/emission-data-webdab/. Accessed on 03.08.2011.
Webster, K.E., Brezonik, P.L., 1995. Climate confounds detection of chemical trends related to acid deposition in upper Midwest lakes in the USA. Water, Air and Soil Pollution 85, 1575–1580.